Population of the giant pairing vibration

M. Laskin, R. F. Casten, A. O. Macchiavelli, R. M. Clark, and D. Bucurescu

On the Population of the Giant Pairing Vibration

M. Laskin,[1, *] R. F. Casten,[1] A. O. Macchiavelli,[2] R. M. Clark,[2] and D. Bucurescu[3]

[1]*Department of Physics, Wright Laboratory, Yale University, New Haven, CT 06520, USA*
[2]*Nuclear Science Division, Lawrence Berkeley National Laboratory, Berkeley, California 94720, USA*
[3]*National Institute for Physics and Nuclear Engineering, R-77125 Bucharest-Magurele, Romania*

Background: The Giant Pairing Vibration (GPV), a correlated two-nucleon mode in the second shell above the Fermi surface, has long been predicted and expected to be strongly populated in two-nucleon transfer cross sections similar to those of the normal Pairing Vibration (PV). Recent experiments have provided evidence for this mode in ^{14,15}C, but despite sensitive studies, it has not been definitively identified either in Sn or Pb nuclei where pairing correlations are known to play a crucial role.

Purpose: Our aim is test whether features inherent to the mixing of bound and unbound levels might account for this and to study the effect in a simple and intuitively clear approach.

Method: We study the mixing of unbound levels in a set of toy models that capture the essential physics of the GPV, along with a more realistic calculation including Distorted Waves Born Approximation (DWBA) transfer amplitudes.

Results: The calculated (relative) cross section to populate a simulated GPV state is effectively low, compared to the case of bound levels with no-widths

Conclusions: The mixing turns out to be only a minor contributor to the weak population. Rather, the main reason is the melting of the GPV peak due to the width it acquires from the low orbital angular momentum single particle states playing a dominant role in two-nucleon transfer amplitudes. This effect, in addition to a severe Q-value mismatch, may account for the elusive nature of this mode in (t, p) and (p, t) reactions.

I. INTRODUCTION

Pair correlations in nuclear motion play a key role in our understanding of the excitation spectra of even-A nuclei, odd-even mass differences, rotational moments of inertia, and a variety of other phenomena [1].

The Hamiltonian describing the motion of independent particles coupled by pairing forces is in second quantization

$$H = \sum_j e_j(a_j^\dagger a_j + a_{\bar{j}}^\dagger a_{\bar{j}}) - G \sum_{j,k} a_j^\dagger a_{\bar{j}}^\dagger a_k a_{\bar{k}} \qquad (1)$$

where the single-particle energies, measured from the Fermi surface, are denoted by e_j, and the single-particle creation operators by $a_j^\dagger$.

It has been predicted that there should be a concentration of strength, with L=0 character, in the high-energy region (10-15 MeV) of the pair-transfer spectrum. This is called the Giant Pairing Vibration (GPV) and is understood microscopically as the coherent superposition of 2p (addition mode) or 2h (removal mode) states in the next major shell $2\hbar\omega$ above (below) the Fermi surface [2]. It is analogous to the well-known pairing vibrational mode [3–5] which involves spin-zero-coupled pair excitations across a single major shell gap. The nature of the GPV is schematically illustrated in Fig. 1, that shows

the solution of the dispersion relation obtained from an RPA approximation of the Hamiltonian in Eq. 1 [2]

$$\frac{2}{G} = F(E) = \sum_j \frac{(2j+1)}{E - 2e_j} \qquad (2)$$

The two bunches of vertical lines represent the unperturbed energy of a pair of particles placed in a given potential. The GPV is the collective state relative to the second major shell. It is analogous to the giant resonances of nuclear shapes which involve the coherent superposition of ph intrinsic excitations.

As in the case of the low-lying PV, the GPV should be populated through pair-transfer reactions, like (t,p) or (p,t), but despite efforts so far it has never been identified [6, 7] with these reactions.

Very recently Ref. [8] reported on an experiment to investigate the GPV mode, using heavy-ion-induced two-neutron transfer reactions on light nuclei. They studied the reactions ^{12}C(^{18}O,^{16}O)^{14}C and ^{13}C(^{18}O,^{16}O)^{15}C at 84 MeV incident laboratory energy. "Bump-like" structures in the excitation energy spectra were identified as the GPV states in ^{14}C and ^{15}C nuclei at excitation energies of $\approx$ 20 MeV. The L=0 nature of these structures and the extracted transfer probabilities appear consistent with the GPV population. It remains as an intriguing puzzle the fact that this mode has not been observed in heavier systems like Sn and Pb isotopes, where the collective effects are expected to be much stronger and for which the low-lying pair excitations are well described by pairing rotations in the Sn's and by pairing fluctuations near the critical point in the Pb's [1, 9].

---

* Present address: Department of Physics, University of Chicago, 929 57th St, Chicago, IL 60637, USA

As it is well known from the theory of 2-nucleon transfer reactions, there is an optimum Q-window for the transfer to occur [10, 11]. In fact, Refs. [11–13] have suggested the use of ^{6}He and ^{11}Li projectiles for which the 2n-transfer reaction Q-value is better matched than in the case of (t,p). Data on ^{6}He on ^{208}Pb exists [14] but the signal of the GPV could be masked by the large probability for break-up of ^{6}He into ^{4}He +2n. More sensitive experiments using these weakly bound projectiles should be pursued.

While the role of the Q-value mismatch is, of course, very relevant, the question we wish to address in this paper is: what is the possible role of mixing of bound and unbound levels in rendering the GPV difficult to observe? To this end we will study and illustrate the often unexpected, and even counter-intuitive, effects of mixing of unbound states using a set of toy models that embody the essential physics. We will show a number of calculations as a function of the number (fraction) of unbound levels, of the mixing matrix elements, of the unperturbed energies, the initial widths, and the interaction strengths. These will show several characteristic and robust features. Following this we will show results from a more realistic (yet still schematic) calculation that brings together several of these elements. At the end, we will bring in aspects of 2-nucleon transfer cross sections, especially the dependence on single-particle orbital angular momenta, that must be convoluted with the coherence of the mixed wave functions to produce estimates for the final cross sections.

$$\hbar\omega_{GPV} \sim 2\hbar\omega_0 - \Omega G \sim \frac{65 MeV}{A^{1/3}}$$
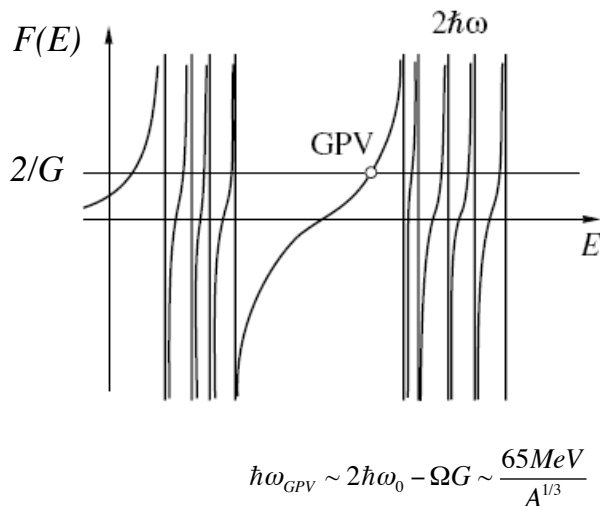
FIG. 1. Schematic of the dispersion relation, Eq. 2, showing the appearance of the collective GPV state and its estimated energy.

Much of the formalism for mixing of bound and unbound levels has been elegantly worked out in papers by von Brentano, Weidenmuller and collaborators [15] which we have relied on extensively. In the next section, we describe the toy calculations and illustrate the results. In the following section we discuss a more realistic calculation and relate it to expected cross sections for exciting the GPV, incorporating estimates of relative form factors for transferring pairs with different angular momenta, from the DWBA. The final section summarizes our conclusions, the main point being that the GPV is indeed greatly diluted in strength but not, in fact, due to mixing.

II. CALCULATIONS WITH TOY MODELS

The paring hamiltonian introduced in Eq. (1) corresponds to a NxN matrix of the form:

$$\begin{pmatrix} e_1 & V_{12} & V_{13} & ... \\ V_{12} & e_2 & V_{23} & ... \\ V_{13} & V_{23} & e_3 & ... \\ ... & ... & ... & ... \end{pmatrix}$$

Much of the essential physics is easily illustrated in Fig. 2, with a schematic 2 x 2 calculation in which one of the initial states has a width. Here we start with two unperturbed levels, separated by 0.4 MeV, positioned at 10 and 10.4 MeV, that mix with an interaction strength [1] of 1 MeV. The calculations show the behavior as a function of varying the initial width for the upper level. On the lower panel in Fig. 2 are the perturbed energies as a function of the initial width of the upper level, and the top panel shows the analogous results for the final widths. The results indicate that, relative to the calculation with no widths (extreme left of the panel), the energy of the lower level rises as the width of the initial level increases. The top panel shows the sharing of the initial width between the two final levels. Notice that, as the initial width grows, the two levels asymptotically approach the initial unperturbed spacing.

As we will see more generally below, there are three characteristic effects of mixing involving unbound levels with widths. First, as with bound levels, the energies repel. Secondly, the larger the widths involved, the less the levels repel. Hence, the final, perturbed, levels are closer together than they would be if there were no widths involved. That is, the lowest level rises relative to the bound situation. This, in fact, was one of the motivations for the present study, namely that, due to this effect, the GPV might lie higher than expected. Thirdly, the final widths are closer together in magnitude than the initial widths. von Brentano [16] has referred to this as *level repulsion and width attraction*. These effects

―――――

[1] Throughout the paper we will refer to this attractive (negative) mixing matrix element as V. See also discussion in Section III.

should make it more difficult to observe the GPV, but it remains to be seen how this translates into the expected collectivity of the GPV and, in turn, into expected cross section.

Next we will discuss the behavior illustrated on Fig. 2 in the more general context of multi-state mixing and show that the conclusions above are robust. We will also encounter some interesting general results and limiting cases.
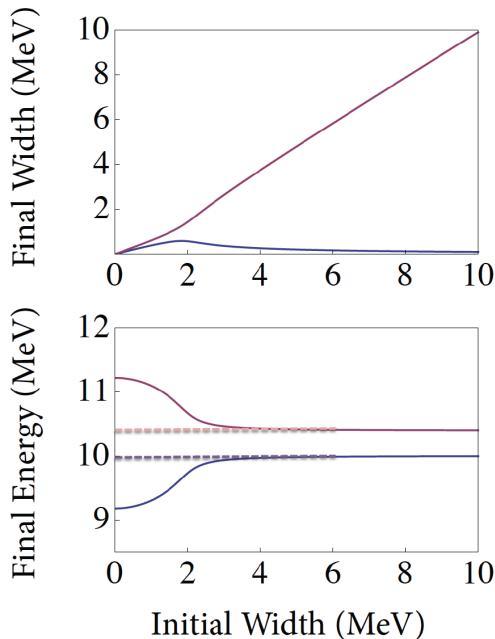
While the energy of an unperturbed GPV may well be fairly near threshold it is highly unlikely that this effect would play a frequent role in different mass regions, with different shells, and different pairing regimes. Therefore, while stressing that care must be taken in cases where it could play a role, the remainder of our calculations will be carried out well above threshold where this effect can be ignored.
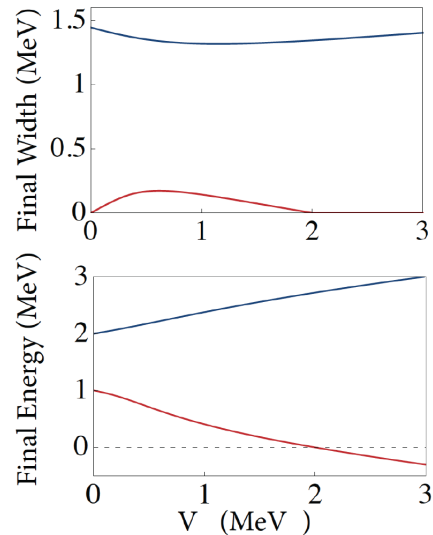

FIG. 2. Results for the mixing of 2 states as a function of the width of the upper level.

FIG. 3. Results for the mixing of 2 states to illustrate the threshold effect on the widths. See also Fig. 2 of [15].

A. Threshold behavior

The above conclusions are robust as long as all levels involved are unbound before and after mixing. However, if the lowest level(s) is pushed below threshold (becomes bound) then, by definition, it cannot have a width and this must be imposed on the calculations. This is best done by embodying a penetration factor into the matrix elements as described in [15]. We will now briefly describe how this modifies the results although, for simplicity, in the rest of this paper we will place all initial levels sufficiently high in energy in our schematic calculations that this effect does not come into play.

We consider again the 2 x 2 case, Figure 3 illustrates the results of a calculation for two levels initially separated by 1 MeV and with the upper one having an initial width of 1.4 MeV. As the mixing increases the lower level decreases in energy. It also obtains an increasing width, however, as the perturbed energy of the lower level approaches threshold (becomes bound) its width must decrease to zero.

B. More levels

Here we will explore the behavior of the mixing calculations as a function of the initial widths and the interaction strengths for cases with different numbers of unperturbed levels with widths. Let us start with a 4x4 calculation to illustrate a general result.

Consider Fig. 4 whose panels show the energy levels with 1 (bottom-right), 2 (bottom-left), 3 (top-right) and 4 (top-left) levels with widths. In each panel, the unperturbed energies are spaced 1 MeV apart at 10,11,12, and 13 MeV. The interaction strength is 1 MeV between all pairs of levels. For the cases with 1,2 or 3 levels with initial widths, the lowest level has no initial width and the other higher levels are successively given widths. For example, for the lower left panel, the levels with initial widths are the second and third levels, and for the upper right panel, the second, third and fourth levels have initial widths.

A generic behavior appears to emerge. The bottom-right panel in Fig 4, with one level with a width, shows a very similar pattern as Fig. 2 for the 2 x 2 case: the final energies of the two levels approach each other, and the unperturbed energies, as the width of the upper level

increases. The upper two levels largely function as spectators.

The panels for which 2 and 3 levels have initial widths shows an interesting behavior. In each case, the highest level with an initial width is "attracted" to the lower level, and the other two levels are again largely spectators. That is, a behavior similar to that in Fig. 2 shows up in the lowest level and in the highest one that has a initial width.

Note that the effect of the widths decreases the more levels having initial widths. This leads to the following interesting and unexpected result: if all levels have identical initial widths one obtains the same results as for the case with no widths, as seen clearly in the top-left panel. The reason is embedded in the idea that the mixing leads to width attraction. That is, the widths after mixing are closer than before. But if all the levels have identical initial widths, the mixing cannot change them and hence cannot have any effect at all.
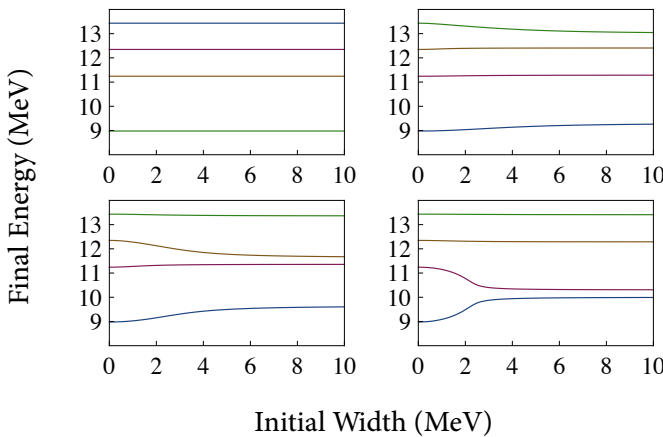

FIG. 4. Results for the mixing of 4 states for different numbers of levels with initial widths. Top-left: 4 levels with widths, top-right: 3 levels, bottom-left: 2 levels, and bottom-right: 1 level. See also text for details.

Mixing calculations with degenerate levels show unique features [17]. In particular, in the simplest case of N bound degenerate levels mixing pairwise with identical matrix elements V, one level is lowered by (N-1)V and all the others rise by V. Here we investigate what happens when some (n) levels are unbound. Figure 5 shows results for a set of N=6 degenerate levels, as a function of the initial widths, for one (top panel) , two (middle panel) , and three (bottom panel) levels with initial widths. The 6 levels are at an energy of 11 MeV and mix with a V=1 MeV matrix element. The far left of each panel corresponds to the bound state case and shows the maximum separation of the perturbed levels. As the initial widths increase the lowest two levels approach each other as we have seen (The other levels remained pinned at their values for the bound state case).

Interestingly, as the number of levels with initial

widths, n, starts to increase, the lowest two perturbed levels are forced closer and closer together, and increasingly so as the initial widths increase. For n = 3, they become degenerate at some value of the initial width and remain so thereafter. This trend does not continue when more than half the levels have initial widths but rather reverses. That is, the calculations with 2 and 4 levels with initial widths are identical, as are those with 1 and 5 or 0 and 6. The closest approach is always when half the levels have widths.

We now explore this situation as a function of the total number N of initial levels. In Fig. 6 we show results for the mixing of N degenerate levels (at 11MeV) and a mixing strength V=1 MeV, when half, n = N/2, of the levels have initial widths. The figure shows results for N = 2, 4, and 6 degenerate levels. The magnitude of the initial widths varies along the abscissa. At the far left, when these widths vanish, the lowest levels are lowered by ((N-1)V) 1, 3, and 5 MeV, respectively, and the other levels rise by (V) 1 MeV. As the initial widths increase the perturbed levels approach each other and become degenerate again when the initial width W = NV. The recovered degeneracy occurs at the average perturbed energy of the upper and lower energy groups,

$$E = E_0 - (N-1)V = E_0 + V - W;$$

C. Coherence and collectivity

Aside from the energies and widths, an important consideration in the observability of the GPV is the coherence in the mixed wave functions. This is expected to enhance the observed cross sections as the different amplitudes for the two-particle transfer operator have the same sign and add coherently. As a measure of the collectivity, we then look at the transfer operator, realizing that a realistic estimate should take into account the kinematic features of the two nucleon transfer cross sections to 0^+ states, by considering a DWBA calculation.

Given a set of single particle orbits $|n\ell j\rangle \equiv |j\rangle$, the wave function of the GPV state can be written:

$$|GPV\rangle = \sum_j \alpha_j |j^2\rangle;$$

The matrix element for the transfer of a pair of L=0 neutrons to the GPV in nucleus $|A_0+2>$ from the ground state of $|A_0>$ is

$$\langle GPV|T|A_0\rangle = \sum_j \alpha_j \langle j^2|T|0\rangle;$$

and the cross section

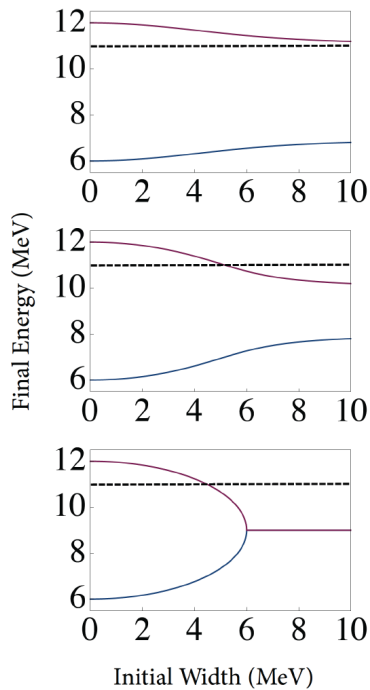$$\sigma(GPV) \propto \langle GPV|T|A_0\rangle^2 = (\sum_j \alpha_j)^2 \sigma_{sp};$$

FIG. 5. Results for the mixing of 6 degenerate levels. The lowest two states are shown as a function of the number of levels with width, top: 1 level with width, middle: 2 levels, and bottom: 3 levels. The other 4 levels remain at 12 MeV. The dashed line indicates the unperturbed energy.
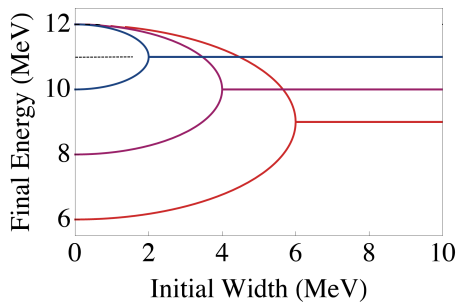

FIG. 6. Results for the NxN mixing case for N/2 levels with widths. Blue: 2 levels, magenta: 4 levels and red: 6 levels. As in Fig. 5, the unperturbed energy is at 11 MeV (dashed line).

with the further assumption that the single particle matrix elements are all approximately equal, $\langle j^2|T|0\rangle^2 \approx \sigma_{sp}$. As we will discuss later, this simplification is not always realistic.

In general, for mixing of unbound states, the amplitudes α_j will be complex $x_j + iy_j$

TABLE I. j^2 levels used in the realistic calculations

Level	Energy (MeV)	Width (MeV)
$s_{1/2}$	14.6	8
$d_{3/2}$	15.4	2.6
$d_{5/2}$	15.9	1.6
$g_{9/2}$	18.0	0.45
$g_{7/2}$	19.5	1.5
$i_{11/2}$	22.0	0.2
$h_{11/2}$	23.6	3.2
$j_{15/2}$	24.5	0.2

$$\sigma(GPV) = ((\sum_j x_j)^2 + (\sum_j y_j)^2)\sigma_{sp};$$

The limiting case of N degenerate levels provide an estimate of the maximum collectivity. With all levels bound, we have $x_j \approx \frac{1}{\sqrt{N}}$ and thus

$$\sigma(GPV) \approx N\sigma_{sp};$$

If the mixing involves unbound levels, and for example $x_j \approx \sqrt{\frac{1}{N} - \delta^2}$ and $y_j \approx \delta$, then again

$$\sigma(GPV) \approx N\sigma_{sp};$$

suggesting that collective effects in the wave function of the GPV do not seem to depend strongly on the mixing with unbound levels.

Rather, and as discussed earlier, the two-nucleon transfer cross sections to 0^+ states depend not only on the coherence of the wave functions but on the specific amplitudes for transfer of angular momentum zero-coupled pairs for different single-particle states. Basically, this reflects the relative amplitudes for the $^1S_0$, 2n amplitude, in the configurations $|(n\ell j)^2, L = 0\rangle$ [18]. These amplitudes depend strongly on the orbital angular momentum ℓ, and the transfer probability could drop by order(s) of magnitude for each increase $\Delta\ell = 2$. Hence the bare cross section at the first maximum of the angular distributions for, say, two nucleons in an $i_{13/2}$ orbit, will be about 4 orders of magnitude less than that for the transfer of two $s_{1/2}$ particles. This effect is likely to be more important in the final cross sections than the detailed collectivity of the final states. The selectivity of different two-particle transfer reactions, such as (t,p), ($^{18}O,^{16}O$), and ($^{14}C,^{12}C$), with respect to detailed microscopic configurations in initial and final target states has recently been investigated in Ref. [19].

III. "REALISTIC CALCULATIONS"

We will now explore these effects in a semi-realistic calculation. For this we consider a GPV arising from the

$2\hbar\omega$ shell on top of the doubly-magic nucleus ^{132}Sn. We do not intend to suggest this case as a potential experiment, the reason for our choice is based on the fact that the neutron single particle levels involved correspond to those of ^{208}Pb above the $N =126$ gap, which give rise to the well know low-lying PV in the Pb isotopes. The $2\hbar\omega$ levels considered are listed in Table 1. The energies and widths have been calculated with the computer code GAMOW [20], and because they are unbound for the ^{132}Sn core their ordering is different than in ^{208}Pb. The matrix diagonalization follows from the methods discussed above using a constant pairing force of the form $G\sqrt{2j_1+1}\sqrt{2j_2+1}$ and $G \approx 20$ MeV/A.

A comment regarding our choice of a constant matrix element is in order. For bound states the $1/A$ dependence reflects the decrease of the matrix element of a short range force with the wave functions overlap, and thus the volume. For the unbound states considered here, the A scaling may not follow and a proper treatment of the two-particle resonant states [21, 22] may actually decrease the matrix elements. In those conditions, we expect to have less mixing and reduced collectivity of the GPV, and in this sense, our results can be considered as a best case scenario.

As an example of the results of these calculations, the real parts of the amplitudes of the 3 lowest states are shown in Fig. 7. The coherent effect of the GPV (lowest state) is clearly seen as all the components have the same sign, while the other states have both positive and negative contributions. Note also that the GPV wave function does not change much with the inclusion of the realistic level widths considered in this example. The GPV is found at an excitation energy of ≈ 10 MeV and a width of ≈ 3.3 MeV.

Once the amplitudes have been determined we use them together with DWBA calculations (using the code DWUCK4 [23]) to estimate the cross-section for the reaction ^{132}Sn(t,p) at $E_{Lab}= 20$ MeV populating the GPV in ^{134}Sn . The calculations were made with standard optical model for tritons [24] and protons [25], and a form-factor for two-neutron transfer in a j^2 configuration [23] for the levels in Table I.

The final result is summarized in Fig. 8 that compares the cross-section as a function of excitation energy for the semi-realistic calculations, to that of the case with no-widths, first folded with a detector resolution of 200 keV and second assuming an overall damping width of 800 keV.

An inspection of these results confirms our qualitative expectations anticipated in previous sections, namely the fact that the introduction of level widths does not much affect the lowering (and collectivity) of the GPV state. The biggest effect could be associated with the width of the GPV, treated properly in the formalism above, that causes a "dilution" of the strength into the background of uncorrelated 0^+ states, due to the role of low ℓ orbitals: the $s_{1/2}$ in our example, and possibly $p_{1/2}$, and $p_{3/2}$ in ^{14,15}C [8], which carry much of the $^1S_0$ strength
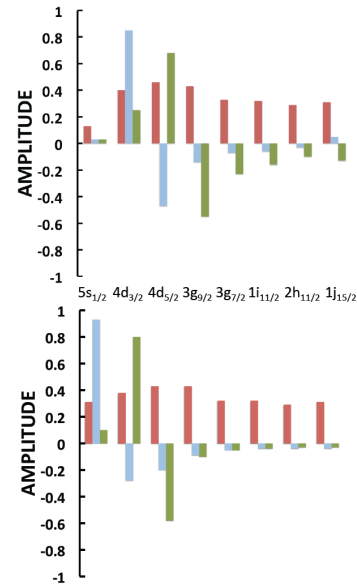

FIG. 7. Wave functions of the lowest 3 states (red, blue and green respectively) obtained from the diagonalization of a pairing force and the levels in Table I. Top: Levels with no-width and Bottom: with width.

but acquire large widths because of their low centrifugal barrier. That is, the most important contributions to the two nucleon transfer cross section are from the same low-spin orbits that acquire large widths when unbound so that any peak structure is severely diluted.

In Ref. [26] the GPV was analyzed within a shell-model formalism in the complex energy plane. In agreement with our results, it was concluded that because of the proper treatment of the continuum the GPV may be too wide to be observed. In contrast, they also find the GPV at higher energy than previously predicted, which could be related to our choice of a constant matrix element discussed above.

We finally note that, while the Q-value mismatch for the (t,p) reaction will affect the overall cross-section, our conclusions relate to the relative values of the cases considered here.

IV. CONCLUSION

As a result of toy model calculations of the mixing of unbound levels we find that, contrary to initial expectations, mixing plays only a small role in lowering these cross sections. More important appears to be the melting of the GPV peak due to the large widths associated with unbound low orbital angular momentum orbits and the fact that these orbits dominate two-nucleon transfer matrix elements. We included these effects in a semi-realistic DWBA calculation of the ^{132}Sn(t,p) reaction, that confirm the model calculations. The "dilution" of
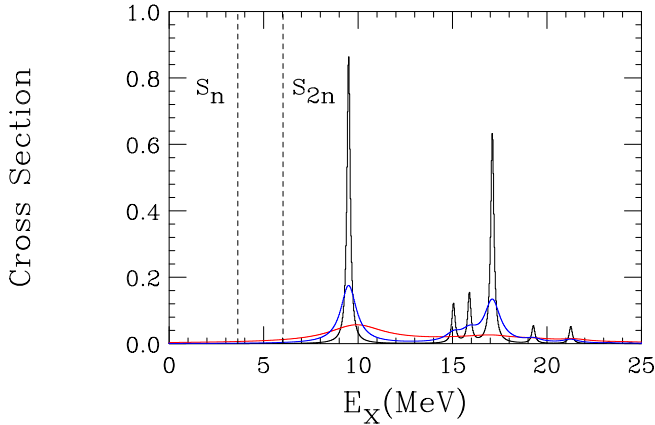
the $^1S_0$ strength in addition to a severe Q-value mismatch [11, 12], may account for the elusive nature of the GPV mode in (t,p) and (p,t) reactions.

Following on the first positive results of Ref. [8], further experimental work, along the lines suggested in Refs. [11, 12], will be required to shed further light on this intriguing question of the population of the GPV. With beams of ^{6}He and ^{11}Li becoming available at the energies and intensities required, the reactions (^{6}He/^{11}Li, α) on Sn or Pb targets appear as the logical next step in these studies.

ACKNOWLEDGMENTS

FIG. 8. Expected relative cross-sections (in arbitrary units) following our semi-realistic calculations (red line), compared to the case of no-widths folded with a detector resolution of 200 keV (black) and a damping width of 800 keV (blue). For reference, the 1-neutron and 2-neutron separation energies are indicated with dashed lines

[1] D. Brink and R. Broglia, Nuclear Superfluidity: Pairing in Finite Systems, Cambridge University Press, Cambridge, 2005
[2] R. A. Broglia and D. R. Bès, Phys. Lett. B 69 129 (1977).
[3] A. Bohr and B. Mottelson, Nuclear Structure, Vol II, World Scientific Publishing Co. 1998.
[4] D. R. Bès and R. Broglia, Nucl. Phys. 80, 289 (1966).
[5] R. A. Broglia, O. Hansen, and C. Riedel, Adv. Nucl. Phys. 6 , 287 (1973) .
[6] G. M. Crawley et al., Phys. Rev. Lett. 39 (1977) 1451.
[7] B. Mouginot et al. Phys. Rev. C83 037302 (2011).
[8] F. Cappuzzello, et al., Nat. Commun. 6:6743 doi: 10.1038/ncomms7743 (2015).
[9] R. M. Clark, et al., Phys. Rev. Lett. 96, 032501 (2006).
[10] R. A. Broglia and A. Winther, Heavy Ion Reactions, Parts I and II, Frontiers in Physics, Westview Press, (2004).
[11] W. vonOertzen and A. Vitturi, Rep. Prog. Phys. **64** (2001) 1247-1337.
[12] L. Fortunato et al., Eur. Phys. J. A 14 (2002) 37 and L. Fortunato, Yad. Fiz. 66 (2003) 1491.
[13] Carlos Dasso, Hugo Sofia, and Andrea Vitturi, Journal of Physics: Conference Series 580 (2015) 012018.
[14] D. Escrig, et al. Nucl. Phys. A792 (2007) 217.

[15] P. von Brentano, R. V. Jolos, and H. A. Weidenmuller, Phys. Lett. B 534 (2002)63.
[16] P. von Brentano, Phys. Rep. 264 (1996) 57.
[17] R. F. Casten, Nuclear Structure from a Simple Perspective, Oxford Studies in Nuclear Physics, 2nd Edition, 2000.
[18] B. F. Bayman and Norton M. Hintz, Phys. Rev. 172, (1968) 1113.
[19] J. A. Lay, L. Fortunato, and A. Vitturi, Phys. Rev. C89, 034618 (2014).
[20] T.Vertse, et al., Comp. Phys. Comm. 27 (1982) 309.
[21] E. Khan, N. Sandulescu, Nguyen Van Giai, and M. Grasso, Phys. Rev. C69 014314 (2004).
[22] R. Id Betan, R. J. Liotta, N. Sandulescu, and T. Vertse, Phys.Rev.Lett. 89 042501 (2002).
[23] P.D.Kunz, DWUCK4 Program Manual. University of Colorado. spot.colorado.edu/~kunz/DWBA.html.
[24] C.M.Perey and F.G.Perey, At. Data Nucl. Data Tables 17(1976)1.
[25] A.J.Koning and J.P.Delaroche, Nucl. Phys. A713 (2003) 231.
[26] G. G. Dussel, R. Id Betan, R. J. Liotta, and T. Vertse, Phys. Rev. C 80, 064311 (2009).